Available online at www.sciencedirect.com
SCIENCE DIRECT®
ELSEVIER
Ocean Modelling 12 (2006) 401–415
Ocean Modelling
www.elsevier.com/locate/ocemod

Sea ice evolution over the 20th and 21st centuries as simulated by current AOGCMs

Olivier Arzel *, Thierry Fichefet, Hugues Goosse

Institut d'Astronomie et de Géophysique Georges Lemaître, Université catholique de Louvain, Chemin du cyclotron, 2, 1348 Louvain-la-Neuve, Belgium

Received 6 May 2005; received in revised form 8 July 2005; accepted 9 August 2005
Available online 8 September 2005

Abstract

Outputs from simulations performed with current atmosphere-ocean general circulation models for the Fourth Assessment Report of Intergovernmental Panel on Climate Change (IPCC AR4) are used to investigate the evolution of sea ice over the 20th and 21st centuries. We first use the results from the "Climate of the 20th Century Experiment" to assess the ability of these models to reproduce the observed sea ice cover changes over the periods 1981–2000 and 1951–2000. The projected sea ice changes over the 21st century in response to the IPCC Special Report on Emission Scenarios A1B are then examined. Overall, there is a large uncertainty in simulating the present-day sea ice coverage and thickness and in predicting sea ice changes in both hemispheres. Over the period 1981–2000, we find that the multimodel average sea ice extent agrees reasonably well with observations in both hemipsheres despite the wide differences between the models. The largest uncertainties appear in the Southern Hemisphere. The climate change projections over the 21st century reveal that the annual mean sea ice extent decreases at similar rates in both hemispheres, and that the reduction in annual mean sea ice volume is about twice that of sea ice extent reduction in the Northern Hemisphere, in agreement with earlier studies. We show that the amplitude of the seasonal cycle of sea ice extent increases in both hemispheres in a warming climate, with a larger magnitude in the Northern Hemisphere. Furthermore, it appears that the seasonal cycle of ice extent is more affected than the one of ice volume. By the end of the 21st century, half of the model population displays an ice-free Arctic Ocean in late summer.

1. Introduction

Since the late 70s, satellite records show a decreasing linear trend in Arctic sea ice extent at a mean rate of about 0.3×10^6 km^2 per decade (Cavalieri et al., 2003). Several numerical experiments display as well a thinning of the Northern Hemisphere (NH) ice pack over the last few decades (Rothrock et al., 2003). The increasing greenhouse gas concentrations associated to human activities is now considered as the main contender to explain this feature (Vinnikov et al., 1999; Houghton et al., 2001; Johannessen et al., 2004), although the role

* Corresponding author. Tel.: +32 104 78501.
E-mail address: arzel@astr.ucl.ac.be (O. Arzel).

1463-5003/$ - see front matter © 2005 Published by Elsevier Ltd.
doi:10.1016/j.ocemod.2005.08.002

of internal variability and natural forcings (solar activity and volcanic eruptions) are still under debate (Bengtsson et al., 2004; Goosse and Holland, 2005). In contrast, observations do not reveal a similar decreasing trend in ice extent in the Southern Hemisphere (SH) over 1978–2002, but rather a slight increase of about 0.2×10^6 km^2 (Cavalieri et al., 2003). This latter trend is however not statistically significant owing to the large interannual variability. The different sea ice responses in the NH and the SH were partly attributed to different oceanic heat uptakes at high latitudes in both hemispheres (Houghton et al., 2001; Flato and Boer, 2001; Goosse and Renssen, 2001).

In the present study, we use the new set of simulations performed with atmosphere-ocean general circulation models (AOGCMs) for the Fourth Assessment Report of Intergovernmental Panel on Climate Change (IPCC AR4) to further examine the sea ice evolution over the 20th and 21st centuries. Our goal is to assess, for both hemispheres, the ability of models to reproduce the observed sea ice changes during 1981–2000 and 1951–2000, and to compare the various sea ice projections over the 21st century. Our analysis is based on model outputs from the "Climate of the 20th Century Experiment" (20C3M) and from the scenario SRES A1B defined by the Special Report on Emission Scenarios (Houghton et al., 2001), which corresponds to a continuous increase of CO_2 concentration over the 21st century until a level of 720 ppm by 2100. The analysis is conducted through the inspection of the simulated trends and standard deviations of sea ice extent and volume as well as the geographical distributions of ice thickness and concentration. The assessment of the model performance over the satellite observing period (1981–2000) is carried out in Section 2, while that over 1951–2000 is presented is Section 3. Section 4 deals with the projected sea ice changes over the 21st century. Concluding remarks are finally given in Section 5.

2. Sea ice evolution over 1981–2000

2.1. Integrated properties

In this section, we focus on the last 20 years of the 20C3M experiment (1981–2000) during which observations are the most reliable. The HadISST dataset (Rayner et al., 2003) is employed to evaluate the ability of models to simulate the geographical distribution of ice concentration, whereas the dataset from the National Snow and Ice Data Center based on a bootstrap algorithm (Comiso, 2002) is used to assess the modeled total sea ice extents. At the time of writing this paper, only 15 AOGCMs (IPSL-CM4, CNRM-CM3, GISS-AOM, GISS-ER, FGOALS-g1.0, CSIRO-Mk3.0, INM-CM3.0, UKMO-HadGEM1, UKMO-HadCM3, MRI-CGCM2.3.2, MIROC3.2 (hires), MIROC3.2 (medres), CGCM3.1 (T47), CCSM3, PCM) had sea ice outputs available on the data distribution center website. Detailed information about these models can be found at http://www-pcmdi.llnl.gov/ipcc/. For each model, we first computed, for each ensemble simulation, the average March and September sea ice extents and the annual mean changes of sea ice extent and volume for both hemispheres over the period 1981–2000. We then averaged, for each model, the results over the ensemble simulations. Note that the sea ice extent is defined here as the total area of oceanic grid boxes with an ice concentration greater than 15%. The results are illustrated in Fig. 1a.

It is first necessary to remind that, unfortunately, models that display small errors in both mean and trend of sea ice extent in a given period are not necessarily better than the others in simulating important processes in polar regions such as radiative transfer or oceanic poleward heat transport for instance. Indeed, the good agreement of a particular model with observations can result from the compensating effect of several processes that are not well represented but whose interactions lead to small model errors in sea ice. An assessment of model quality would thus require much more comprehensive analyses that the ones proposed here.

Since the FGOALS-g1.0 model produces ice extents that are much larger than the observed ones in both hemispheres, its results are shown for completion in Figs. 1 and 3, but are not taken into account in the analysis that follows. Fig. 1a indicates that the multimodel average ice extents in March and September are in reasonable agreement with observations in both hemispheres. In the NH, the multimodel average overestimates the observations by almost 1.0×10^6 km^2 in March, but agrees very well with the observed coverage at the end of the melt season (September). In the SH, the amplitude of the seasonal cycle of the ice extent is somewhat overestimated over 1981–2000. There, the multimodel average ice extent is too large by about 2×10^6 km^2 in September, and too weak by about 0.6×10^6 km^2 in March. In late Arctic wintertime, 10 models

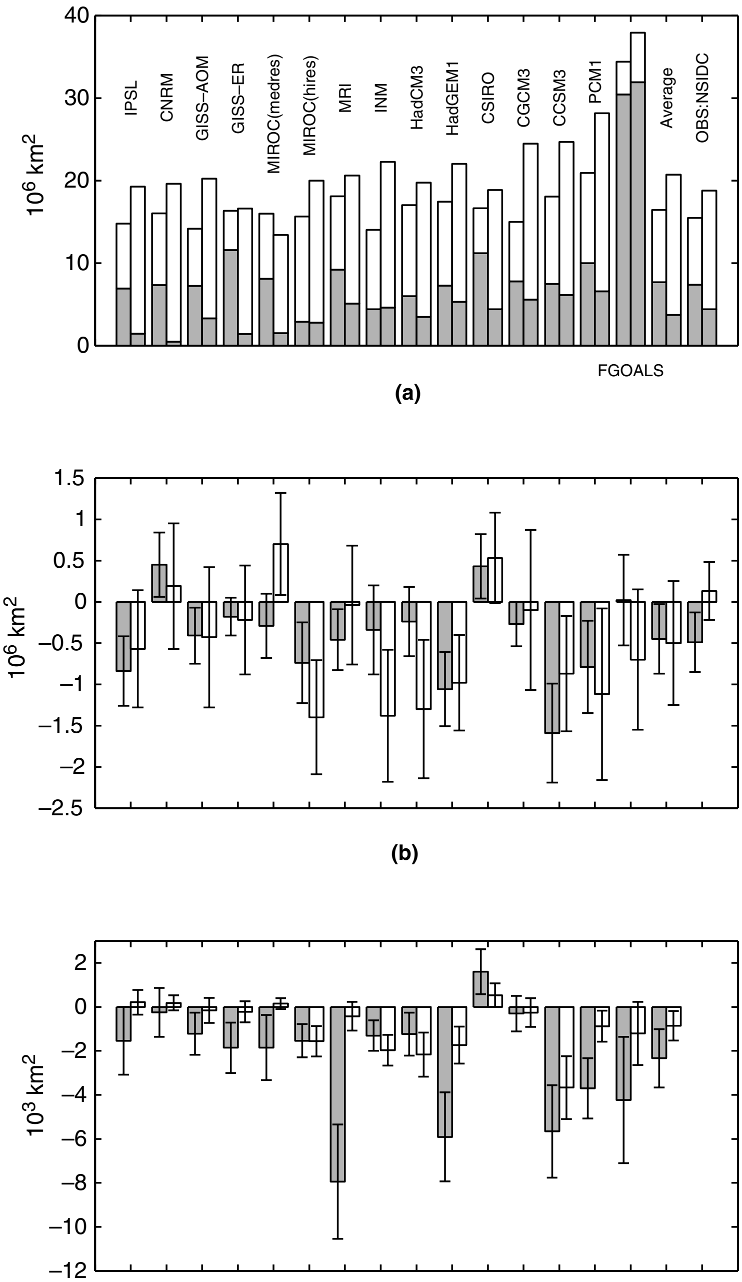

Fig. 1. Arctic and Antarctic sea ice extent and volume averaged over 1981–2000 and their changes. The changes are computed as the differences between values at years 1981 and 2000 computed from the linear trend. For each model, the left (right) bar corresponds to Arctic (Antarctic), (a) mean ice extent. The white shading represents to the absolute value of the ice extent difference between March and September, whereas the gray shading indicates the ice extent at the end of the melt season (September for the NH and March for the SH); (b) change in annual mean sea ice extent over the whole period and corresponding standard deviation for Arctic (gray) and Antarctic (white); (c) change in annual mean sea ice volume over the whole period and corresponding standard deviation for Arctic (gray) and Antarctic (white). The observations are derived from the National Snow and Ice Data Center (NSIDC) dataset using the bootstrap algorithm (Comiso, 2002). The model FGOALS-g1.0 was excluded from the model average.

reproduce quite well the observed sea ice extent within a range of 10%, the MIROC3.2 (hires) model being the closest to the observational value with an error of about 1%. In late Arctic summertime, seven models have errors of about or less than 10% relative to the observations. The models that have relative errors smaller than 10% in both late summer and late winter in the NH are the IPSL-CM4, CNRM-CM3, GISS-AOM, MIROC3.2 (medres) and CGCM3 models, meaning that these models capture well the amplitude of the seasonal cycle of Arctic sea ice extent. The CCSM3 model has a realistic Arctic ice extent in late summer, but overestimates the observations by about 16% in late winter. In contrast, the CSIRO-Mk3.0 and GISS-ER models are close to observations in late winter and produce too large an ice extent in late summer. The INM-CM3.0 and MRI-CGCM2.3.2 models respectively underestimates and overestimates the Arctic sea ice cover throughout the year. As mentioned before, the MIROC3.2 (hires) model is very close to the observations in late Arctic wintertime. Nevertheless it underestimates the observed sea ice extent by about 60% in September. The UKMO-HadCM3 model produces realistic Arctic ice extent in March but underestimates by 18% the observational value in late summer. Finally, the UKMO-HadGEM1 model is very close to observations in late winter and slightly overestimates the sea ice extent in late summer (error of about 12%). In the SH, only the INM-CM3.0 and CSIRO-Mk3.0 models have errors smaller than 10% relative to the observational climatology in late summer. The IPSL-CM4, CNRM-CM3, GISS-ER and MIROC3.2 (medres) models underestimate the observed summer Antarctic ice extent by more than 60%. In late Antarctic wintertime, the models are generally much closer to observations than in late summer, and seven models show relative errors smaller than 10%. Furthermore, note that the CSIRO-Mk3.0 model is the only one having relative errors of less than 10% in both late winter and late summer (0.45% in March and 0.37% in September).

In order to assess the model differences in simulating the sea ice extent in both hemispheres, we calculated the multimodel standard deviations of sea ice extent with respect to the multimodel averages over the period 1981–2000. It appears that the agreement between models is better in winter than in summer for both hemispheres, and is generally better in the NH than in the SH. This hemispheric asymmetry might be due to the low stratification of the Southern Ocean. A small difference between models in the representation of the vertical structure of the water column, caused for instance by differences in both horizontal and vertical mixing, could thus have a large impact on the vertical oceanic flux and ultimately on the ice cover. By contrast, in the Central Arctic, as the ocean stratification is strong, small model errors have a much weaker impact on the heat flux at the ice-ocean interface. Moreover, the sea ice in the Southern Ocean is not constrained by land as in the Arctic and is therefore more free to evolve.

Fig. 1b compares the simulated changes in sea ice extent and corresponding standard deviations with the observations over 1981–2000. The sea ice changes correspond to the differences of sea ice extent between 1981 and 2000 estimated from the linear trend which is computed from the annual mean anomalies. The ability of IPCC AR4 models to simulate the observed annual mean decreasing trend in Arctic sea ice area is investigated in Zhang and Walsh (2005). Although we have focused in our study on sea ice extent, we obtained the same results as these authors based on sea ice area analysis. In the NH, the multimodel ensemble mean change is about -4.3×10^5 km^2 or -2.15×10^5 km^2 per decade, which is very close to the observational estimate derived from NSIDC, about -2.4×10^5 km^2 per decade. This leads to a decreasing trend of -1.8% per decade over 1981–2000 with respect to the multimodel ensemble mean of annual mean ice extent. Moreover all the models reproduce a decrease of annual mean sea ice extent in the Arctic, except the CNRM-CM3 and CSIRO-Mk3.0 models which show positive trends over 1981–2000. It should be noted that the change in annual mean ice extent is statistically significant at the 90% confidence level since it is slightly greater than one standard deviation both in the multimodel ensemble mean and observations. It seems then unlikely that natural variability be responsible for this decreasing trend. In the SH, the multimodel average annual mean ice extent experiences a decrease of 4.7×10^5 km^2 (1.6% of the mean per decade) that is very similar to the sea ice change in the NH over 1981–2000. The CNRM-CM3, MIROC3.2 (medres) and CSIRO-Mk3.0 models display an increase of annual mean Antarctic ice cover over 1981–2000, while the others exhibit a decrease. Furthermore, note that seven models (FGOALS-g1.0 excluded) give a decrease larger than 5×10^5 km^2 in the SH. Although the observations indicate a slight increase of about 1.3×10^5 km^2 in the SH, it is still difficult to assess the agreement between models and observations since the standard deviation of ice extent is larger than the change both in models and observations over 1981–2000.

Examining the seasonal changes over 1981–2000, we found that, in the NH, the strongest decrease occurs in September and the weakest in March in models as well as in the real world (see e.g., Chapman and Walsh, 1993). The multimodel ensemble displays however a change (not shown) that overestimates the observations by about 3 $\times 10^5$ km^2 in September and slightly underestimates the observed change in March (−2.9 vs. −2.6 $\times 10^5$ km^2). In the SH, the main model-data difference appears in September: the multimodel average shows an Antarctic sea ice extent reduction of -7×10^5 km^2, whereas the observations exhibit an increase of 4.1 $\times 10^5$km^2. Finally, the agreement between models in simulating sea ice extent changes is slightly better in the NH than in the SH, but remains quite weak since the annual mean multimodel differences are of the order of 120% in the NH and 141% in the SH.

The interannual variability of sea ice extent that emerges from models is also an useful measure of assessment of AOGCMs. In the NH, the multimodel ensemble mean standard deviation of annual mean sea ice extent is 4.2×10^5 km^2, close to the value derived from NSIDC (3.6×10^5 km^2). The INM-CM3.0, CCSM3 and PCM1 models overestimate the observed interannual variability by more than 50%, while the GISS-ER and CGCM3 models underestimate this variability by 36% and 25%, respectively. In contrast, in the SH, all the models strongly overestimate the amplitude of the interannual variability, the multimodel error being about of 114% higher than the observational estimate.

Overall, these results point out the difficulty of climate models to reproduce the observed climatology in the SH. Moreover, none of the 15 climate models used here are able to capture simultaneously the observed mean, trend and interannual variability of sea ice extent in both hemispheres with an error of less than 10% over 1981–2000.

The agreement between models and observations regarding the total sea ice volume is difficult to assess since ice thickness variability is only known from submarine-based observations which do not cover the entire Arctic Ocean. Because of the spatio-temporal sampling of these data, a large uncertainty persists about the sea ice volume changes over the last few decades. Rothrock et al. (1999) found a 40% decrease in Central Arctic sea ice volume since the late 50s, whereas Winsor (2001) found no significant change over the 90s. Hilmer and Lemke (2000) and, more recently, Rothrock and Zhang (2005) estimated that the Arctic annual mean ice volume declined at a rate of about 0.89×10^3 km^3 per decade (4% of the mean volume per decade) since the 60s with their ocean-sea ice models forced with NCEP/NCAR reanalysis atmospheric data. Here, we explore the sea ice volume changes simulated by current AOGCMs over 1981–2000 in order to better quantify the transient sea ice behavior. The total changes in annual mean volume are depicted in Fig. 1c for both hemispheres. The 14 models used in the present study indicate a decrease in annual mean ice volume of about -2.2×10^3 km^3 over 1981–2000 (-1.1×10^3 km^3 per decade) in the NH. This corresponds to a decrease of about 4.9% of the mean volume per decade and thus is similar to the estimate of Hilmer and Lemke (2000) and Rothrock and Zhang (2005). Note however that the spread of modeled sea ice volume trends is large and ranges from +2 to −11% of the mean volume per decade over 1981–2000, the median trend being −4.2% per decade. In the SH, the multimodel average shows a decrease in annual mean ice volume of about -0.8×10^3 km^3 or −2.9% of the mean per decade over 1981–2000, about 60% of the one of the NH. The modeled sea ice volume trends range from +3.3% to −10.5% per decade, the median trend being −2.4% per decade.

In contrast to the multimodel annual mean sea ice extent changes that are very similar in both hemispheres (−1.8% per decade in the NH and −1.6% per decade in the SH), the multimodel annual mean ice volume reduces almost 70% more rapidly in the NH than in the SH over 1981–2000 (−4.9% per decade vs. −2.9% per decade respectively). We will see that a similar behavior is observed in response to the increase in greenhouse gases concentration over the 21st century. Furthermore, the standard deviation of sea ice volume as well as that of ice extent can vary by a factor 2 between models in both hemispheres. As for the sea ice extent changes, the model uncertainty in sea ice volume changes is slightly lower in the NH than in the SH, but remains strong enough (106% in the NH against 134% in the SH for the multimodel differences of annual mean volume changes).

Following Rind et al. (1995), we have tried to relate the sea ice changes to time-averaged sea ice properties over 1981–2000. No clear relationship could be found except between mean ice extent in the Arctic and its variability in summer. We found that the larger the mean summer ice extent averaged over 1981–2000, the smaller the ice extent summer standard deviation over the same period, with a correlation coefficient of about 0.75. This could be due to the Arctic Ocean geometry (C. Bitz, personal communication, 2005). In summer, the main variability in ice extent north of 70°N is presently mainly observed over continental shelves. This could be reproduced by model that have reasonable or too small an ice cover. By contrast, for the models that display too extensive an ice cover, the ice reaches the coast of Siberia, Alaska and North Canada every year. As a consequence, only limited regions in the Barents Sea or in the Nordic Sea exhibit significant variability, leading to a smaller variance than in models with less extensive ice cover. The opposite relationship is found for the Antarctic in summer (correlation coefficient of about 0.65), where the sea ice is not constrained by land. There, the amplitude of sea ice variability is thus proportional to the mean ice extent.

2.2. Geographical distribution over 1981–2000

In this section, we examine the geographical distribution of sea ice as simulated by 14 models (FGOALS-g1.0 excluded) and compare how well the sea ice edge location produced by the models agrees with observations over the period 1981–2000. We follow the same approach as Flato (2004) and determine the percentage of model population that has ice (with a concentration greater than 15%) in a given grid cell. In order to compare the results from the different models, all the sea ice outputs have been sampled on a 360×180 regular

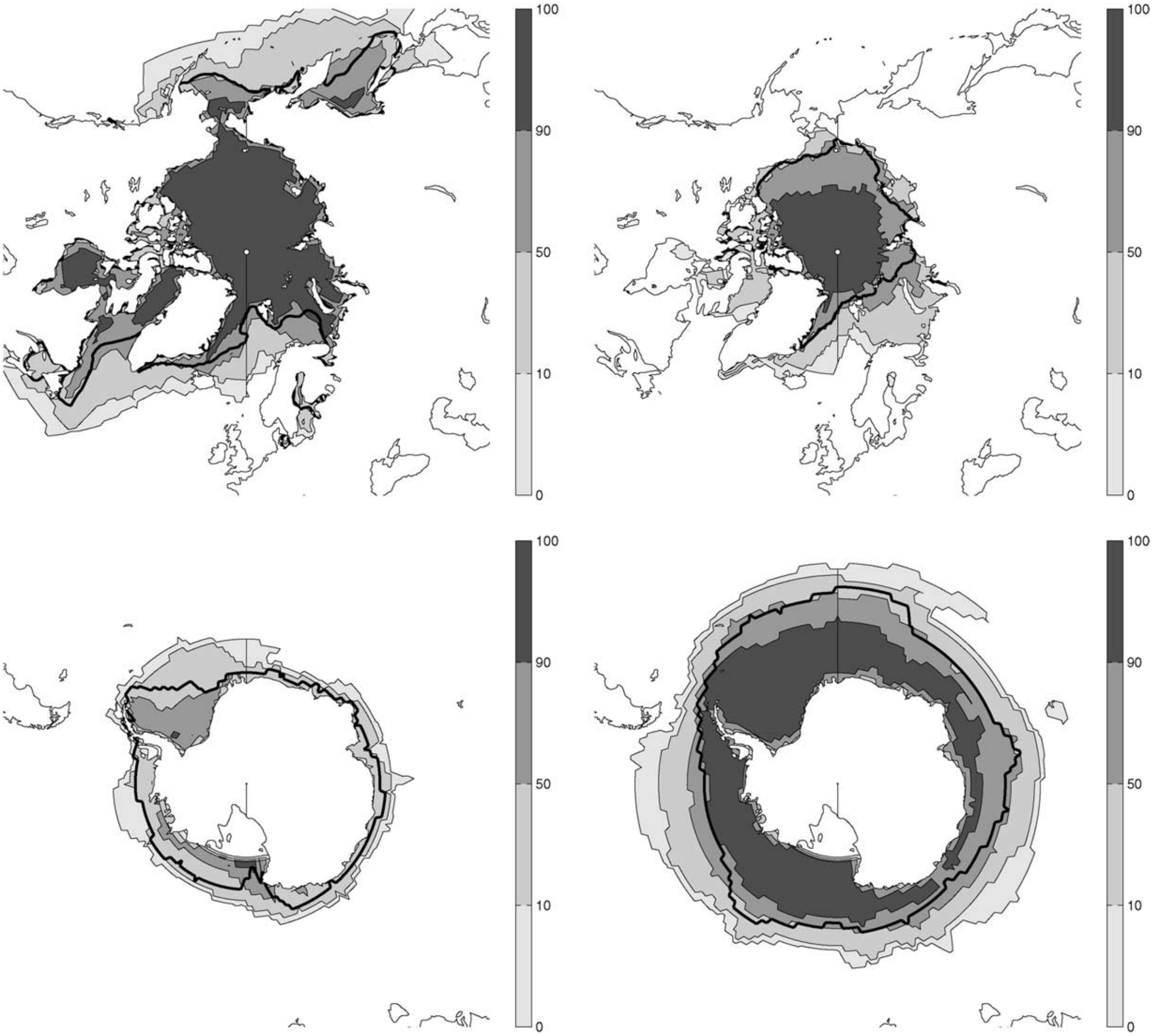

Fig. 2. Range of sea ice extent in the model simulations over 1981–2000 (20C3M experiment). Shading indicates the percentage (%) of models that have ice in average over the period 1981–2000 in March (left) and September (right) for both hemispheres. The analysis is based on 14 models (FGOALS-g1.0 excluded). The observed sea ice edge (thick black line) is based on the HadISST dataset (Rayner et al., 2003).

grid. The spatial patterns of the monthly averages of sea ice cover over 1981–2000 for March and September are shown in Fig. 2 for both hemispheres. The 50% contour corresponds to the median sea ice edge.

In the NH, the ensemble modeled median sea ice edge agrees reasonably well with the observed one (thick black line) in March as well as in September. The distributions of ice cover in late winter in the NH indicate that between 10% and 50% (depending on the precise location) of the models have the Labrador Sea and the Greenland–Iceland–Norvegian Seas partly ice-covered, and that more than 50% of the AOGCMs overestimate the sea ice extent in the southern part of the Barents Sea. This prevents oceanic heat loss to the atmosphere in these areas, which plays an important role in winter oceanic convection. In the SH, the simulated median sea ice edge location lies slightly poleward of the observed one in March, mainly off the Amundsen Sea and in the Weddell Sea. In September, the agreement with the observations is reasonable, but the simulated median sea ice edge lies slightly southward off the Amundsen Sea. This indicates that the amplitude of the seasonal cycle of sea ice extent is generally overestimated by the models in the Amundsen Sea. Note also that the area in which more than 90% have ice during March in the SH is very small, confined in the Ross Sea, suggesting a large disagreement between models in late summer there. Furthermore, the spread amongst the simulated sea ice edge is large in the NH in both the North Pacific and North Atlantic sectors. In the SH, the spread is large at all longitudes in late winter, and mainly off the Weddell Sea in late summer. But, as already shown in Fig. 1b, the range of variability is large in some models, mainly in the SH, making difficult to compare accurately models with observations. Furthermore, as the differences between models is large, it should be stressed that the relatively good agreement between the median ice edge and observations results from the averaging of some models with too small an ice extent and models with too much large an ice extent.

3. Integrated properties of sea ice extent over 1951–2000

Given the significant low-frequency variability of sea ice extent and thickness in both hemispheres, it is necessary to check if the conclusion deduced from the period for which the best data are available (i.e., 1981–2000) are also valid if we analyse a longer period. The analysis of the climatology over this period leads to similar conclusions about the various model strengths and deficiencies. In particular, the multimodel ensemble mean sea ice extent over 1951–2000 is close to observations in both hemispheres during the full seasonal cycle (FGOALS-g1.0 excluded).

The multimodel ensemble mean trend in the NH and SH are similar over 1951–2000, and are -1.28×10^5 km^2 per decade and -1.23×10^5 km^2 per decade, respectively. In the NH, this corresponds to a decrease of 6.4×10^5 km^2 over 1951–2000, slightly greater than the multimodel ensemble mean standard deviation (4.6×10^5 km^2). The modeled Arctic sea ice extent trend is then statistically significant at the 90% confidence level but, in contrast to that simulated over 1981–2000, strongly underestimates the observed sea ice change that is about $-18.2 \pm 6.3 \times 10^5$ km^2 from the HadISST dataset (Rayner et al., 2003). However, Rayner et al. (2003) cautioned that their reconstruction provides only a general indication of sea ice variations before the 1970s. Observations derived from Chapman and Walsh (1993) display a decreasing linear trend of -1.9×10^5 km^2 per decade over 1953–1998. This leads to a change of -8.7×10^5 km^2 over 1953–1998, that is slightly greater then the present multimodel ensemble mean change over 1951–2000 (-6.4×10^5 km^2). In the SH, the models show a decrease of 6.2×10^5 km^2 over 1951–2000 that is still smaller than the standard deviation of the ensemble (8.4×10^5 km^2) as over the period 1981–2000. The multimodel ensemble mean sea ice trend in the SH is then not statistically significant in contrast to the observations that show a significant decrease of $-25.0 \pm 8.9 \times 10^5$ km^2 over 1951–2000. It should be stressed that most of this decrease occurs over 1973–1977 in HadISST (-21.5×10^5 km^2), and the models do not reproduce such a large sea ice reduction over this 5-year period.

The multimodel annual mean sea ice volume trend is -0.80×10^3 km^3 per decade in the NH, almost 5 times that of the SH (-0.17×10^3 km^3). In the NH, this leads to a decrease of -4.0×10^3 km^3 over 1951–2000, which is significant at the 95% confidence level. Furthermore, this downward trend is -3.8% of the mean annual volume per decade over 1951–2000, and is very close to the value of Rothrock and Zhang (2005) (-4% per decade). In the SH however, the annual mean sea ice volume change (-0.85×10^3 km^3, corresponding to a trend of -1.5% per decade) is not statistically significant since the multimodel ensemble mean shows a standard deviation of 0.77×10^3 km^3 over 1951–2000.

4. Projected future sea ice changes in the SRES A1B scenario

4.1. Integrated properties

A large number of numerical studies suggest that the Arctic sea ice extent might substantially decrease over the 21st century in response to the increasing atmospheric concentrations of greenhouse gases (e.g., Flato, 2004; Hu et al., 2004; Gregory et al., 2002). In the Southern Ocean, however, the range of sea ice responses between models is much larger (Flato, 2004). We investigate the changes in sea ice extent and volume simulated by 13 AOGCMs driven by the A1B scenario for greenhouse gas and sulfate aerosol concentrations. The PCM1 model is not taken into consideration since its sea ice outputs were unavailable for the SRES A1B scenario on the data distribution center website at the time of writing this paper, and the FGOALS-g1.0 model was excluded from our analysis for the same reason as before. The annual mean or monthly changes in sea ice extent and volume are taken as the difference between the averages over the period 2081–2100 from the A1B scenario and the averages over the period 1981–2000 from the 20C3M experiment. The results are summarized in Table 1. These anomalies are expressed as a difference (%) with respect to averaged conditions over 1981–2000.

In the NH, the reduction in annual mean ice volume is about twice the decrease in annual mean ice extent in agreement with the results of Gregory et al. (2002) obtained using the UKMO-HadCM3 model under several warming scenarios. By contrast, the ice volume reduction is slightly greater than the ice extent change in the SH. The difference in the rate of change of sea ice volume with respect to sea ice extent between the NH and SH could be attributed to the different initial ice pack thicknesses. Bitz and Roe (2004) demonstrated that sea ice experiences a growth-thickness negative feedback that is much stronger for thinner ice than for thicker ice. This thermodynamic feedback implies that thinner ice does not need to thin as much than thicker ice to increase its growth rate. Through this mechanism, the changes in ice thickness in the SH would be smaller than the ones of the NH since sea ice is usually thinner in the SH than in the NH. The changes of ice volume would then be smaller in the SH than in the NH since the rates of changes of sea ice extent are observed to be similar in both hemispheres.

Changes in seasonal cycle might also occur in the future (see Table 1). We found that the Arctic ice extent reduction is almost four times greater in summer (September, −61.7%) than in winter (March, −15.4%). In the SH, the ratio of sea ice extent reduction between March and September is smaller and amounts at about 2.5. These results indicate that (i) the amplitude of the seasonal cycle of sea ice extent increases in response to the increasing atmospheric concentrations of greenhouse gases and (ii) that this amplitude increases more rapidly in the NH than in the SH. In contrast to sea ice extent, the sea ice volume reduction ratio between summer and winter is of the same order in both hemispheres (2.1 against 1.7). Moreover, these sea ice volume reduction ratios between summer and winter are smaller than those associated with ice extent changes in both hemispheres. This shows that the projected seasonal changes of sea ice are mainly in extent rather than in volume. By contrast, the annual mean projected sea ice change is mainly in ice volume as mentioned before (see Table 1). Finally, note that half of the models (CNRM-CM3, MIROC3.2 (medres), MIROC3.2 (hires), UKMO-HadCM3, UKMO-HadGEM1, CCSM3) display an ice-free Arctic at the end of the summer season by 2100 as reported in some previous studies (Gregory et al., 2002; Johannessen et al., 2004).

Fig. 3 shows the simulated changes in annual mean sea ice extent and volume between the last 20 years of the 21st century and the last 20 years of the 20th century. The multimodel average indicates that the sea ice extent changes are of the same order in both hemispheres, about -3×10^6 km^2 in agreement with Flato (2004), corresponding to a decrease of about 25% (Table 1) with respect to the average over 1981–2000. By contrast,

Table 1
Multimodel average relative changes (%) of sea ice extent (SIE) and volume (SIV) between the periods 2081–2100 and 1981–2000 for March, September and the annual mean (AM) in both hemispheres (FGOALS-g1.0 excluded)

	Arctic			Antarctic		
	March	September	AM	March	September	AM
SIE	−15.4	−61.7	−27.7	−49.0	−19.1	−24.0
SIV	−47.8	−78.9	−58.8	−58.1	−27.4	−33.7

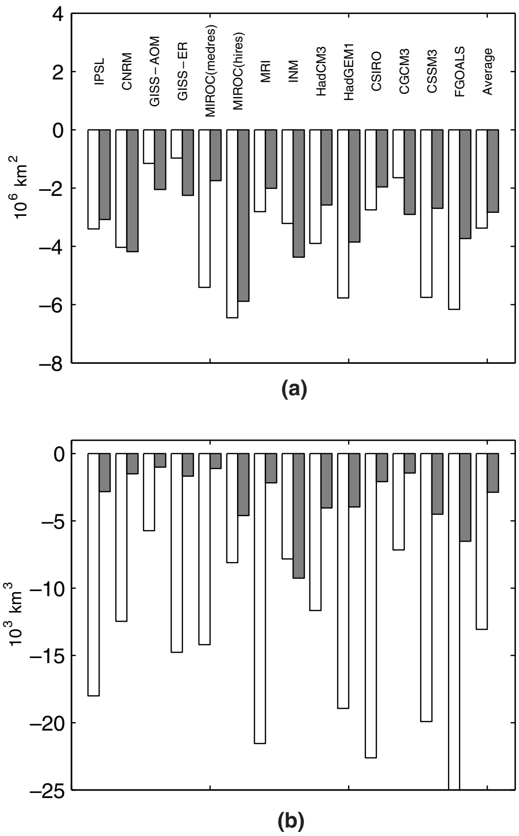

Fig. 3. Changes in Arctic and Antarctic annual mean sea ice extent (a) and volume (b) at the end of the 21st century. For each model the left (right) bar represents Arctic (Antarctic). The model FGOALS-g1.0 was excluded from the model average.

the multimodel average of annual mean sea ice volume changes displays a much larger reduction in the NH than in the SH (13.1×10^3 against 2.9×10^3 km^3). This is primary due to the much larger volume in the Northern Hemisphere at the end of the 20th century, and to the growth-thickness negative feedback documented by Bitz and Roe (2004).

In order to provide a measure of the uncertainty in simulating the sea ice extent and volume changes over the 21st century, we computed the ratio between the multimodel standard deviation of sea ice changes and the multimodel average of sea ice changes for both ice extent and volume. A small percentage indicates a narrow distribution of model results. We found that the model responses in sea ice volume are in better agreement in the NH than in the SH (44.3% vs. 78.8% on annual average). The largest model uncertainty occurs in late summer in the SH (119%) and the smallest in late Arctic wintertime (41%). In contrast, the model uncertainty is somewhat smaller in the SH than in the NH regarding the annual mean sea ice extent responses (42.9% in the SH and 53.6% in the NH).

4.2. Geographical distributions

In this section, we first examine the geographical distribution of the projected sea ice cover averaged over 2081–2100. The multimodel average sea ice cover responses over 2081–2100 are illustrated in Fig. 4. This figure has been constructed following Flato (2004) and displays the fraction of the model population that have ice at a given grid point. The observed sea ice edge averaged over 1981–2000 from the HadISST dataset (thick, black line) is represented for comparison. Overall, the most noticeable difference with the average ice climatology over 1981–2000 (Fig. 2) is that the area in which more than 90% of the model population have ice has totally disappeared in summer in both hemispheres. By contrast, during wintertime, this area has decreased

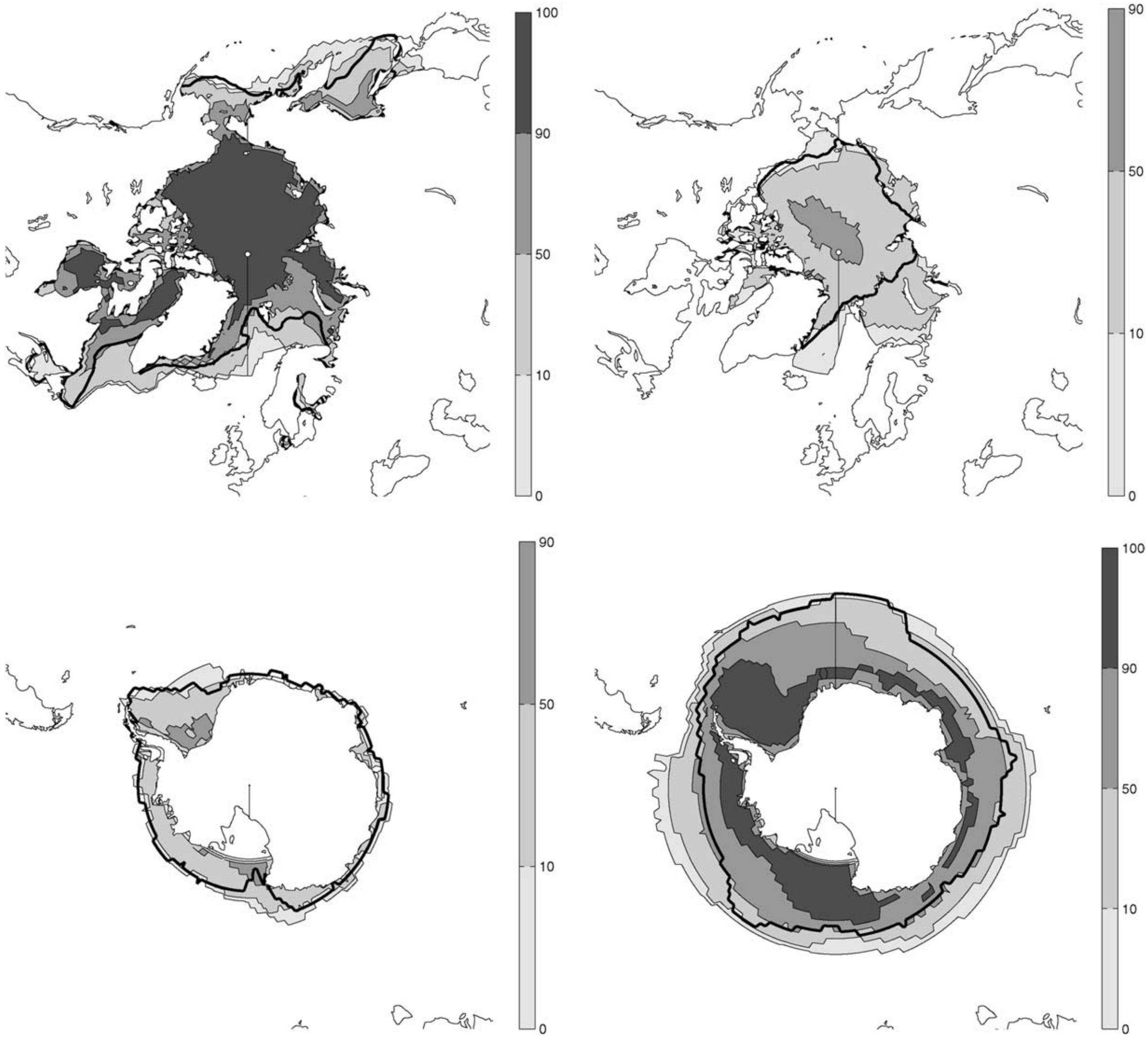

Fig. 4. Percentage (%) of models which have ice on average over the period 2081–2100 (experiment A1B) in March (left) and September (right) for both hemispheres (FGOALS-g1.0 excluded). The analysis is based on 10 models. For comparison, the thick black line represents the observed sea ice edge averaged over 1981– 2000, derived from the HadISST dataset (Rayner et al., 2003).

much less in the NH than in the SH (−17.1% vs. −38.5% respectively). These results suggest that under the considered warming scenario, ice can survive in winter because temperatures are still cold enough in polar regions. Indeed, the simulated median sea ice edge in late winter averaged over 2081–2100 is not very far from the observed one averaged over 1981–2000, except in the North Pacific sector and in the Atlantic sector of the Southern Ocean. Using the version 2 of the Community Climate System Model (CCSM2) subjected to a 1% increase in CO_2, Bitz et al. (in press) showed that the small changes in the wintertime position of the sea ice edge at the time of a CO_2 doubling is mostly due to the decrease in ocean heat flux convergence that defeats the increase in surface radiative forcing.

An analysis of the multimodel standard deviation of absolute sea ice concentration changes (difference between 2081–2100 and 1981–2000) in the NH reveal that the largest difference occurs in the northern parts of the Barents, Labrador, Bering and Okhotsk Seas with values of about 50% in late winter. In late Arctic summertime, the multimodel differences are large from the north of the Canadian Archipelago and north of the Greenland coast to the Central Arctic with values of about 65%. In late Antarctic summertime, the multimodel standard deviation of absolute sea ice concentration changes are the largest in the western part of the

Weddell Sea (45%). In late winter, the largest differences occur in the western part of the Pacific and Atlantic sectors, and in the eastern part of the Indian sector (50%). Note that the spatial pattern of the multimodel standard deviation of absolute sea ice concentration changes is very similar to that of sea ice concentration changes in late winter as well as in late summer in both hemispheres. Moreover, the multimodel standard deviation is generally larger than the sea ice concentration change in these specific regions. There is therefore a large uncertainty in simulating the sea ice concentration changes at the regional scale.

Comparison of sea ice draft data between 1993–1997 and 1958–1976 indicates that the mean ice thickness at the end of the melt season in the Central Arctic has decreased from 3.1 m to 1.8 m (Rothrock et al., 1999). The simulations used here show that the thinning continues throughout the 21st century. For each model, we computed the relative monthly mean ice thickness difference between 2081–2100 and 1981–2000 with respect to 1981–2000. These differences were calculated when the initial mean thickness over 1981–2000 was greater than 15 cm. The relative differences were then averaged, for each grid point, over the model population that displayed ice initially (1981–2000) in order to avoid biased changes. The results are shown in Fig. 5 for March and September in both hemispheres.

In addition to some zones along the sea ice edge where ice disappears (100% decrease in ice thickness), the relative winter ice thickness changes are the largest in the Barents Sea, just east of Svalbard, with a thinning of

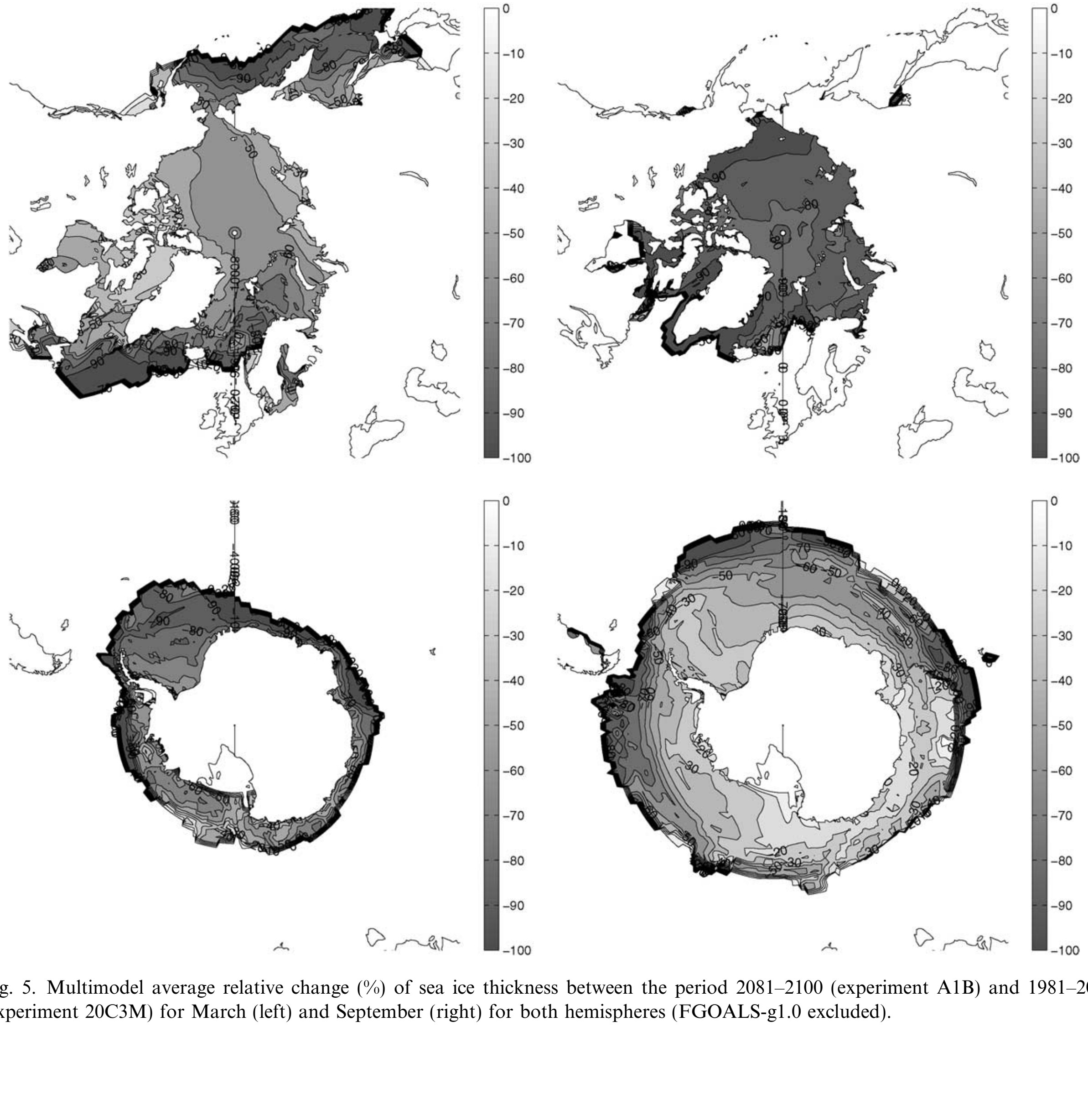

Fig. 5. Multimodel average relative change (%) of sea ice thickness between the period 2081–2100 (experiment A1B) and 1981–2000 (experiment 20C3M) for March (left) and September (right) for both hemispheres (FGOALS-g1.0 excluded).

about 70–80% with respect to 1981–2000. This might be due to an enhanced oceanic poleward heat transport of waters originating from the North Atlantic into the Arctic, as proposed earlier by Holland and Bitz (2003). The second maximum of ice thickness change occur in the Central Arctic (between −50% and −60%) and bear some resemblance with the mean ice thickness field (not shown), in agreement with Flato (2004). The ice thickness changes during September in the Central Arctic are more homogeneous and also larger (−70% to −80%) than for March as anticipated by the sea ice volume changes given in Table 1. In this case, the largest thinning is observed north of the Bering Strait in the Chukchi Sea (−90%). Rigor and Wallace (2004) argued that the recent depletion of sea ice cover in the Chukchi and Beaufort Seas during the summers 2002 and 2003 is due to a delayed response to a high index of Arctic Oscillation (AO) that occurred in 1989–1995. It would then be useful to determine how the sea ice balance (ice export and ice melting/growing) is modified in this region under warming scenario, and how it is related to changes in the atmospheric circulation, but this is out the scope of this paper. Overall, the relative ice thickness changes are smaller in the SH than in the NH. However, in March, the changes are large in the eastern part of the Weddell Sea (about −75%). In contrast to the CMIP2 climate change simulations described by Flato (2004), we found a significant negative trend in the central Weddell Sea (−60%) for March. In September, significant changes are noticed in the Atlantic and Pacific sectors of the Southern Ocean (−30% to −50%). In the Atlantic sector, the smallest changes appear in the central Weddell Sea (−30%) in September. Note that the Antarctic sea ice thickness changes do not show obvious positive correlation with the mean initial ice thicknesses (1981–2000, not shown) as already noted by Flato (2004).

The largest multimodel standard deviation of ice thickness changes lies in a region extending from the north of the Canadian Archipelago to the Central Arctic with values up to 100% there with respect to ice thickness changes. In the SH, the main model differences in simulating the sea ice thickness changes are concentrated in the Weddell Sea and in the eastern part of the Amundsen Sea, with values of up to 100% there. Furthermore, the spatial pattern of multimodel standard deviation of ice thickness changes is somewhat independent of the season in both hemispheres.

Flato (2004) found that models that simulate thick ice in their control integration exhibit less warming than those with thin ice in the NH. He found an opposite relationship in the SH. We therefore explore here the possible relationships between ice properties averaged over 1981–2000 and the sea ice extent and volume changes over the 21st century. These changes correspond to differences between averages over 2081–2100 and 1981–2000. We find that, in late summer, the larger the ice extent for present-day conditions (1981–2000), the smaller the relative changes of sea ice extent with respect to initial ice extent with a correlation of about 0.68 in the NH and 0.58 in the SH, and the smaller the relative changes of sea ice volume with a correlation of about 0.66 in the NH and only 0.43 in the SH. According to this analysis, two model behaviors should coexist in the Arctic during summertime: on the one hand, models with large summertime ice extent for present-day conditions which display small fraction of sea ice changes, and, on the other hand, models with small summertime ice extent for present-day conditions which are very sensitive to increasing greenhouse gas concentrations leading to an ice-free summer Arctic at the end of the 21st century. By contrast, the relationship between initial ice extent and absolute ice extent change is only significant in late summer in Antarctic and opposite to that between initial ice extent and relative extent changes: the larger the initial ice extent, the larger the absolute ice extent change with a correlation of 0.83. No statistically significant relationships is found between the initial ice thickness (1981–2000) and other sea ice physical quantities, except that the larger the summertime initial ice thickness (1981–2000), the larger the ice volume changes. The correlation coefficients are 0.95 in the NH and 0.81 in the SH. In annual mean, the correlation coefficients between initial ice thickness and absolute volume change is 0.75 in the NH and 0.68 in the SH.

5. Concluding remarks

In this study, we have discussed results about the sea ice behavior over the 20th and 21st centuries from the new set of simulations performed with state-of-the-art AOGCMs for the IPCC AR4. In particular, we have assessed the ability of these models to reproduce the observed evolution of the sea ice cover over 1981–2000 using the outputs from the 20CM3 experiment. We have also examined the projected sea ice changes over the 21st century in response to the IPCC SRES A1B scenario for greenhouse gas and sulfate aerosol concentrations.

Despite the large model disagreement over 1981–2000, the multimodel average Arctic ice extent and its trend are in reasonable agreement with satellite passive-microwave observations. In the SH, the models generally overestimate the amplitude of the seasonal cycle of sea ice extent and display, on average, a negative trend over 1981–2000. This contrasts with the observations that indicate rather a slight increase. However, the large interannual variability in models as well as in observations makes difficult to compare the simulated sea ice extent trends with observations in the SH over 1981–2000. We found that, in summer, the larger the mean ice extent averaged over the period 1981–2000, the smaller the standard deviation of ice extent during the same period in the NH, but the opposite in the SH. We found that the multimodel annual mean sea ice extent changes are very similar in both hemispheres over 1981–2000 (-1.8% per decade in the NH and -1.6% per decade in the SH). By contrast, the multimodel annual mean ice volume decreases almost 70% more rapidly in the NH than in the SH over 1981–2000 (-4.9% per decade vs. -2.9% per decade respectively).

The climate change projections conducted with the models indicate that the sea ice decline will continue over the 21st century and half of the model population exhibit an ice-free summer Arctic by 2100. We found that the annual mean Arctic and Antarctic sea ice extents experience a similar decrease of about 25% over 2081–2100 with respect to average coverage over 1981–2000. Our results also show that the sea ice volume reduction is about twice that of sea ice extent in the NH but of the same order of the ice extent change in the SH. The thermodynamic growth-thickness negative feedback documented by Bitz and Roe (2004) is invoked to explain those differences of sea ice behavior between the NH and the SH over the 21st century. Examining the seasonal cycle changes, we showed that the amplitude of the seasonal cycle of sea ice extent will increase in both hemispheres, but at a greater rate in the NH. Although the projected annual mean Arctic sea ice changes over the 21st century are mainly in ice volume, we find that the simulated sea ice seasonal changes are mainly in extent rather than in volume. Future investigations will be needed to determine how the sea ice changes are related to dynamic and thermodynamic processes.

The models show large differences in sea ice cover over the period 1981–2000. The simulated Arctic mean sea ice extents in March over 1981–2000 range from about 14×10^6 km^2 to 20×10^6 km^2, whereas the observed coverage averaged over the same period is about 15×10^6 km^2. The differences between models are more apparent at the end of the melt season. The modeled Arctic mean sea ice extents in September over 1981–2000 range from about 3×10^6 km^2 to 11×10^6 km^2, while the observations show a mean September ice extent about 7×10^6 km^2 averaged over 1981–2000. The multimodel differences are even more pronounced in the Southern Ocean in winter and summer. Despite the improvement of the representation of sea ice physics in AOGCMs since the IPCC Third Assessment Report (Houghton et al., 2001), there is still a large uncertainty in simulating the present-day sea ice climatology. This points out the difficulties of climate models to deal with high latitude processes. Thus, from this observation, caution has to be taken regarding the reliability of the simulated future sea ice changes, particularly at the regional scale. Furthermore, sensitivity experiments will be needed in order to determine to what extent model uncertainty depends on sea ice physics and also other aspects of climate (Liu et al., 2003), such as oceanic mixing for instance.

Finally several studies have shown that the response of the Southern Ocean to an increase in atmospheric greenhouse gas concentrations is delayed compared to other regions (Goosse and Renssen, 2001; Bi et al., 2001; Goosse and Renssen, 2005) mainly because of the large thermal inertia of the Southern Ocean. As the models used here indicate similar decreasing rates of sea ice extent in both hemispheres, it is possible that the decrease simulated during the late 20th and 21st centuries is related to the increase in the forcing that occurred since the beginning of the 20th century. Nevertheless, in this framework, as argued by Goosse and Renssen (2005), the initial conditions might play a role in the model behavior since they could have an influence on the sea ice cover in the Southern Ocean for more than 200 years. Sensitivity of the model response to the starting date of the simulations would then be useful to examine the influence of initial conditions on the variations of sea ice cover in the SH over the 21st century.

Acknowledgements

Valuable comments on this study were received from C.M. Bitz and G.A. Schmidt. We acknowledge the international modeling groups for providing their data for analysis, the Program for Climate Model Diagnosis and Intercomparison (PCMDI) for collecting and archiving the model data, the JSC/CLIVAR Working

Group on Coupled Modelling (WGCM) and their Coupled Model Intercomparison Project (CMIP) and Climate Simulation Panel for organizing the model data analysis activity, and the IPCC WG1 TSU for technical support. The IPCC Data Archive at Lawrence Livermore National Laboratory is supported by the Office of Science, US Department of Energy. This work was conducted within the European project ENSEMBLES (ENSEMBLE-based Predictions of Climate Changes and their Impacts). The Bootstrap sea ice extents were obtained through the National Snow and Ice Data Center (NSIDC), University of Colorado, Boulder. This study is supported by the Federal Science Policy Office (Belgium), contracts EV/10/7D and EV/10/9A and the Action Concerté Incitative Changement Climatique (project Changement Climatique et Cryosphère) from the French Ministry of Research. H. Goosse is a research associate with the Belgian National Fund for Scientific Research.

References

Bengtsson, L., Semenov, V.A., Johanessen, O.A., 2004. The early twentieth-century warming in the Arctic. A possible mechanism. Journal of Climate 17, 4045–4057.

Bi, D., Budd, W.F., Hirst, A.C., Wu, X., 2001. Collapse and reorganisation of the Southern Ocean overturning under global warming in a coupled model. Geophysical Research Letters 28 (20), 3927–3930.

Bitz, CM., Roe, G.H., 2004. A mechanism for the high rate of sea ice thinning in the Arctic Ocean. Journal of Climate 17, 3623–3631.

Bitz, C.M., Holland, M.M., Hunke, E.C., Moritz, R.E., in press. On the maintenance of the sea-ice edge. Journal of Climate.

Cavalieri, D.J., Parkinson, C.L., Vinnikov, K.Y., 2003. 30-year satellite record reveals contrasting Arctic and Antarctic decadal sea ice variability. Geophysical Research Letters 30 (18). doi:10.1029/2003GL018931.

Chapman, W.L., Walsh, J.E., 1993. Recent variations of sea ice and air temperature in high latitudes. Bull. Am. Meteorol. Soc 74, 33–47.

Comiso, J.C., 2002. Bootstrap sea ice concentrations from Nimbus-7 SMMR and DMSP SSM/I. Boulder: National Snow and Ice Data Center. Digital media.

Flato, G.M., 2004. Sea-ice and its response to CO_2 forcing as simulated by global climate models. Climate Dynamics 23, 229–241.

Flato, G.M., Boer, G.J., 2001. Warming asymmetry in climate change simulations. Geophysical Research Letters 28, 195–198.

Goosse, H., Holland, M., 2005. Mechanisms of decadal and interdecadal Arctic variability in the Community Climate System Model CCSM2. Journal of Climate 18 (17), 3552–3570.

Goosse, H., Renssen, H., 2001. A two-phase response of the Southern Ocean to an increase in greenhouse gas concentration. Geophysical Research Letters 28, 3469–3472.

Goosse, H., Renssen, H., 2005. A simulated reduction in Antarctic sea-ice area since 1750: implications of the long memory of the ocean. International Journal of Climatology 25, 569–579. doi:10.1002/joc.1139.

Gregory, J.M., Stott, P.A., Cresswell, D.J., Rayner, N.A., Gordon, C., Sexton, D.M.H., 2002. Recent and future changes in Arctic sea ice simulated by the HadCM3 AOGCM. Geophysical Research Letters 29 (24). doi:10.1029/2001GL014575.

Hilmer, M., Lemke, P., 2000. On the decrease of Arctic sea ice volume. Geophysical Research Letters 27, 3751–3754.

Holland, M.M., Bitz, C.M., 2003. Polar amplification of climate change in coupled models. Climate Dynamics 21, 221–232.

Houghton, J.T., Ding, Y., Griggs, D.J., Noguer, M., van der Linden, P.J., Dai, X., Maskell, K., Johnson, C.A., 2001. Climate change 2001. The scientific basis. Contribution of Working Group I to the Third Assessment Report of the Intergovernmental Panel on Climate Change. Cambridge University Press, Cambridge, UK.

Hu, Z.-Z., Kuzmina, S.I., Bengtsson, L., Holland, D.M., 2004. Sea-ice change and its connection with climate change in the Arctic in CMIP2 simulations. Journal of Geophysical Research, 109. doi:10.1029/2003JD004454.

Johannessen, O.M., Bengtsson, L., Miles, M.W., Kuzmina, S.I., Semenov, V.A., Alek-seev, G.V., Nargurnyi, A.P., Zakharov, V.F., Bobylev, L., Perttersson, L.H., Hasselmann, K., Cattle, H.P., 2004. Arctic climate change—Observed and modeled temperature and sea ice variability. Tellus 56A, 328–341.

Liu, J., Schmidt, G.A., Martinson, D., Rind, D.H., Russell, G.L., Yuan, X., 2003. Sensitivity of sea ice to physical parameterizations in the GISS global climate model. Journal of Geophysical Research 108 (C2). doi:10.1029/2001JC001167.

Rayner, N.A., Parker, D.E., Horton, E.B., Folland, C.K., Alexander, L.V., Rowell, D.P., Kent, E.C., Kaplan, A., 2003. Global analyses of sea surface temperature, sea ice, and night marine air temperature since the late nineteenth century. Journal of Geophysical Research 108 (D14). doi:10.1029/2000JC000542.

Rigor, I.G., Wallace, J.M., 2004. Variations in the age of Arctic sea-ice and summer sea-ice extent. Geophysical Research Letters, 31. doi:10.1029/2004GL019492.

Rind, D., Healy, R., Parkinson, C., Martinson, D., 1995. The role of sea ice in $2 \times CO_2$ climate model sensitivity. Part II: Hemispheric dependencies. Geophysical Research Letters 24, 1491–1494.

Rothrock, D.A., Yu, Y., Maykut, G.A., 1999. Thinning of the Arctic sea ice cover. Geophysical Research Letters 26, 3469–3472.

Rothrock, D.A., Zhang, J., 2005. Arctic ocean sea ice volume: What explains its recent depletion? Journal of Geophysical Research, 110. doi:10.1029/2004JC002282.

Rothrock, D.A., Zhang, J., Yu, Y., 2003. The Arctic ice thickness anomaly of the 1990s: a consistent view from observations and models. Journal of Geophysical Research 108 (C3). doi:10.1029/2001JC001208.

Vinnikov, K.Y., Robbock, A., Stouffer, R.J., Walsh, J.E., Parkinson, C.L., Cavalieri, D.J., Mitchell, J.F.B., Garrett, D., Zakharov, V.F., 1999. Global warming and northern hemisphere sea ice extent. Science 286, 1934–1937.

Winsor, P., 2001. Arctic sea ice thickness remained constant during the 1990s. Geophysical Research Letters 28, 1039–1042.

Zhang, X., Walsh, J.E., 2005. Toward a seasonally ice-covered Arctic Ocean: Scenarios from the IPCC AR4 model simulations. Journal of Climate, submitted for publication.